The Effect of Imposed Drying on Parameterized Deep Convection

ADAM H. SOBEL

Department of Applied Physics and Applied Mathematics, and Department of Earth and Environmental Sciences, Columbia University, New York, New York

GILLES BELLON*

Department of Applied Physics and Applied Mathematics, Columbia University, New York, New York

(Manuscript received 18 August 2008, in final form 2 December 2008)

ABSTRACT

This paper examines the influence of imposed drying, intended to represent horizontal advection of dry air, on parameterized deep convection interacting with large-scale dynamics in a single-column model framework. Two single-column models, one based on the NASA Goddard Earth Observing System general circulation model version 5 (GEOS5) and the other developed by Bony and Emanuel, are run in weak temperature gradient mode. Drying is imposed by relaxation of the specific humidity field toward zero within a specified vertical layer. The strength of the drying is controlled by specifying either the relaxation time scale or the vertically integrated drying tendency; results are insensitive to which specification is used.

The two models reach very different solutions for the same boundary conditions and model configuration. Even when adjustments to the boundary conditions and model parameters are made to render the precipitation rates similar, large differences in the profiles of relative humidity and large-scale vertical velocity persist. In both models, however, drying in the middle troposphere is more effective, per kg m^{-2} s^{-1} (or W m^{-2}) of imposed drying, in suppressing precipitation than is drying in the lower troposphere. Even when compared at equal relaxation time (corresponding to weaker net drying in the middle than lower troposphere), middle-tropospheric drying is comparably effective to lower-tropospheric drying. Upper-tropospheric drying has a relatively small effect on precipitation, although large drying in the upper troposphere cannot be imposed as a steady state because of the lack of moisture there. Consistent with the other model differences, the gross moist stabilities of the two models are quite different and vary somewhat differently as a function of imposed drying, but in both models the gross moist stability increases as the drying is increased when it is less than around 30 W m^{-2} and located in the middle troposphere. For lower-tropospheric drying, the gross moist stability either decreases with increased drying or increases more slowly than for middle-tropospheric drying.

1. Introduction

The occurrence and intensity of deep convection are sensitive to the environmental profile of free tropospheric humidity (e.g., Parsons et al. 1994; Yoneyama and Fujitani 1995; Mapes and Zuidema 1996; Derbyshire et al. 2004). It is becoming widely recognized that a correct representation of this sensitivity is important for convective parameterization schemes in numerical models. There is evidence that inadequate sensitivity to environmental humidity is at least partly responsible for a range of biases in climate models, both in the climatological mean (e.g., Biasutti et al. 2006; Bretherton 2007) and in transient variability, such as the Madden–Julian oscillation (e.g., Tokioka et al. 1988; Lin et al. 2006).

The humidity–convection interaction is manifest in observed statistical relationships between precipitation and column-averaged saturation deficit or other measures of the relative humidity profile (e.g., Sherwood 1999; Sherwood and Wahrlich 1999; Raymond et al. 2003, Bretherton et al. 2004; Peters and Neelin 2006; Cetrone and Houze 2006). These correlations represent

* Current affiliation: Centre National de Recherches Météorologiques, Météo-France/CNRS, Toulouse, France.

Corresponding author address: Adam Sobel, Columbia University, Dept. of Applied Physics and Applied Mathematics, 500 W. 120th St., Rm. 217, New York, NY 10027.
E-mail: ahs129@columbia.edu

DOI: 10.1175/2008JAS2926.1

both the influence of environmental humidity on convection and the influence of convection on environmental humidity. Humidity influences convection through entrainment of environmental air into updrafts and the evaporation of condensate. Humidity also influences convection by direct fueling, as atmospheric boundary layer (ABL) humidity controls the buoyancy of updrafts, and by the entrainment of free tropospheric environmental air into updrafts. Convection influences humidity by consuming ABL humidity, moistening the upper troposphere by detrainment of water vapor and condensate that is susceptible to evaporation, and inducing large-scale ascent and moisture convergence. It is difficult to disentangle these different processes in observations, but useful information comes from looking at the different relationships between convection and humidity as observed at different vertical levels.

Because convective mass fluxes originate near the surface, we expect that environmental humidity at low levels—the boundary layer and the lower portion of the free troposphere—will act as an important control on deep convection. On the other hand, we expect that environmental humidity in the upper troposphere is largely a by-product of convection (or its absence) because convective updrafts reach their ends in the upper troposphere. By the time parcels reach that point, the convection is already deep by definition, so it is too late for entrainment of dry air to prevent deep convection from developing, and most of the precipitation that is likely to form from those parcels has already done so. Both the deep convective moistening and the radiatively induced drying at the top of the troposphere are rapid, so that upper-level humidity is bimodal, reflecting either the presence or absence of convection (Brown and Zhang 1997; Zhang et al. 2003). The bimodality becomes weaker at lower levels to which shallow or midlevel convection, which is more frequent than deep convection, is able to penetrate. Observational studies using time-lagged statistics to infer causality support the intuitive picture of lower-tropospheric humidity influencing convection, whereas upper-tropospheric humidity more passively responds to convection (Sherwood 1999; Sherwood and Wahrlich 1999; Straub and Kiladis 2002, 2003; Sobel et al. 2004).

In the middle of the troposphere, there must be a transition in which environmental humidity goes from having a significant causal influence on convection to being more passively determined by convection, but we do not know the nature of this transition. At what level does it occur, and how rapidly? Is it similar for all deep convective events or does it differ depending on environmental conditions or the structure of the convective system? To what extent can environmental humidity be both a cause and effect of deep convection simultaneously?

These questions motivate this study. We perform a set of calculations using single-column models with parameterized convection. Drying tendencies are imposed in different vertical layers, and the response of the model precipitation and related fields is examined as a function of the strength of the drying and the altitude at which it is applied. This strategy allows us to influence the humidity at selected levels without entirely disabling any feedback between moisture and convection (as would occur, for example, if we were to simply prescribe the humidity profile and keep it fixed). The use of parameterized convection prohibits us from making strong statements about the extent to which the results tell us about nature, but we view the results as posing hypotheses worthy of further consideration. The fact that some aspects of the sensitivity to imposed drying are similar in the two models despite large differences in other aspects of the solutions lends support to this view.

2. Models

a. GEOS5

This model, derived directly from the National Aeronautics and Space Administration (NASA) Goddard Earth Observing System general circulation model (GCM), version 5 (GEOS5), is similar to that described in Sobel et al. (2007) except for the numerical scheme used within the convective parameterization for the vertical advection by compensating subsidence. In Sobel et al. (2007), a first-order upwind scheme was implemented, whereas here we use a centered scheme, which ensures a better conservation of column-integrated moist static energy. The GEOS5 includes a relaxed Arakawa–Schubert parameterization of convection (Moorthi and Suarez 1992) and the radiation scheme of Chou and Suarez (1999). Detailed documentation describing the GEOS5 GCM and its physical parameterizations may be found online (at http://gmao.gsfc.nasa.gov/systems/geos5).

b. Bony–Emanuel model

We use the model of Bony and Emanuel (2001), who developed the cloud parameterization used in the model. The model uses the convection scheme of Emanuel (1991) as further developed by Emanuel and Zivkovic-Rothman (1999). The radiation parameterizations are due to Fouquart and Bonnel (1980) and Morcrette (1991). Further description of the model can be found in Bony et al. (2008). The model is run in pressure coordinates with 46 vertical levels, with a vertical resolution of 25 hPa in the troposphere.

3. Experimental design

The model is run in "weak temperature gradient" (WTG) mode, as in Sobel and Bretherton (2000) and Chiang and Sobel (2002) [both of which used the earlier version of the Massachusetts Institute of Technology (MIT) single-column model—namely, that developed by Rennó et al. (1994a,b)]. An essentially similar but not identical method was used in the cloud-resolving model studies of Raymond and Zeng (2005) and Raymond (2007). Briefly, in the free troposphere the temperature tendency due to vertical advection of potential temperature is assumed to exactly balance the net diabatic tendency due to convection and radiation. The total temperature tendency is thus assumed to be zero, and the free tropospheric temperature does not change throughout the model integration. The vertical velocity (ω, in pressure coordinates) is diagnosed interactively as that consistent with the cancellation of adiabatic cooling (heating) and diabatic heating (cooling). The resulting vertical velocity is used to compute the vertical advection of moisture, thus determining the implicit moisture convergence. In the boundary layer, chosen somewhat arbitrarily to be the layer between the surface and 850 hPa, the original prognostic temperature equation is solved, and the vertical velocity is computed by linear interpolation between the lowest free tropospheric level and the surface, where $\omega = 0$ is assumed.

With each model, we first produce a temperature sounding by running the model in its standard mode (not WTG), with $\omega = 0$ imposed at all levels, to radiative–convective equilibrium (RCE) over a sea surface temperature of 301 K. The surface wind speed is set to 7 m s^{-1} and solar insolation is set to 400 W m^{-2} with a constant solar zenith angle of zero, and thus no diurnal cycle. The resulting RCE temperature profiles are shown in Fig. 1. The difference between the two profiles is largest in the lower to middle troposphere, where the GEOS5 model approaches 2 K warmer than the MIT model at some levels. The GEOS5 model is warmer than the MIT model by 0.5–1 K in the upper troposphere, and slightly cooler near the surface.

The RCE temperature and humidity sounding from each model is used as input to the same model in WTG mode. The humidity profile serves as an initial condition; as the model runs, the humidity varies freely. The same is true of the temperature field below 850 hPa. Above 850 hPa, the temperature profile remains constant and thus is the same throughout each run of each model (although the two models use different temperature profiles, each taken from its respective RCE state). SST is then varied from one calculation to the next to produce drier or rainier model solutions. Sobel et al. (2007) showed that for a range of boundary conditions (essentially, as long as SST is large enough that deep convection is possible for a given free tropospheric temperature profile), the GEOS model in this configuration has two equilibria, one in which deep convection occurs and one in which it does not. The MIT model has the same behavior (not shown). Here, we focus on the influence of imposed drying on convection and therefore consider only the precipitating equilibrium. In both models, precipitation is an increasing function of SST, but the functions are quite different in the two models, as shown in Fig. 2. The MIT model, when run with the same parameters used to generate the RCE, is quite dry, both by comparison to the GEOS5 model and in the sense that it does not reach a precipitation rate equal to that in the RCE state (about 5 mm day^{-1}) until the SST is significantly (~1.7 K) higher than that for which the RCE was obtained. This behavior, shown by the curve labeled "control MIT" in the figure, is quite different than that found by Sobel and Bretherton (2000) in the Rennó et al. (1994a,b) model but is somewhat similar to that found by Raymond and Zeng (2005) in their cloud-resolving model. The GEOS5 model's behavior is strongly in the opposite sense, with the precipitation at an SST of 301 K being much larger than the RCE precipitation obtained at that SST.

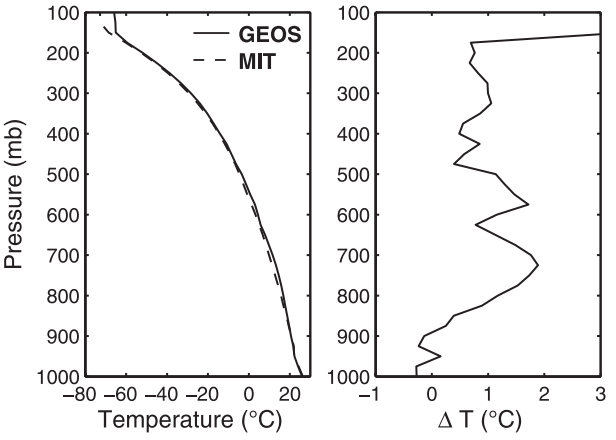

FIG. 1. (left) Radiative–convective equilibrium temperature profiles from the GEOS5 model, the MIT model, and (right) the difference, GEOS5 minus MIT.

Our interest here is on the influence of imposed drying in different vertical layers. To compare this influence in the two models, it is desirable to start with similar model solutions. We wish those solutions to be fairly strongly precipitating because we will apply an imposed drying of varying strength and evaluate the reduction in precipitation that occurs; a rainier solution for zero drying allows a larger dynamic range in the imposed drying. We choose values around 25 mm day^{-1}.

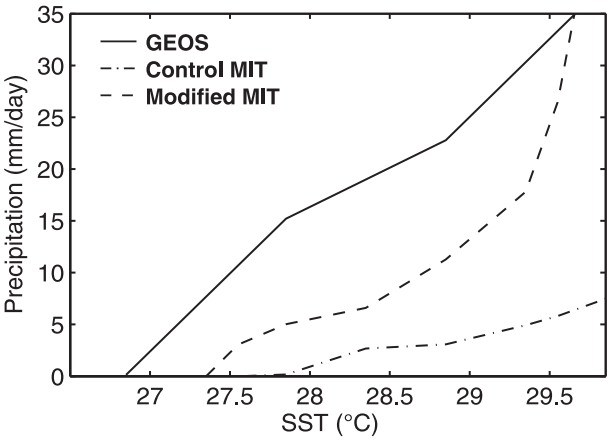

FIG. 2. Precipitation as a function of SST in the GEOS5 model, the control MIT model (the same one used to generate the RCE in Fig. 1), and the modified MIT model (the one used in all calculations presented below). See text for details.

In judging the relevance of these solutions to the real atmosphere, these rain rates should not be compared to observed climatological or even monthly mean rain rates because these typically include periods of no rain, whereas our solutions are steady. It is probably better to view our solutions as representative of shorter periods. As a daily rain rate, for example, 25 mm day^{-1} is not particularly extreme.

To obtain such a rainy solution in the GEOS5 model, we increase the SST to 302 K, one degree warmer than that used to obtain the RCE. To obtain precipitation similar to that of the GEOS5 model in the calculation with no imposed drying, we increase the SST in the MIT model relative to that used in GEOS5 by 0.7 K, to 302.7 K, and also change the values of three parameters in the convection scheme (see appendix). The resulting model, called the ''modified MIT model'' in Fig. 1, is used in all calculations described below.

The parameter changes in the modified MIT model render it different from that used to produce the RCE sounding. This compromise is made so that we do not have to make the SST difference between the two models even larger still to get similar precipitation rates. Sensitivity tests show that the results from the MIT model are not qualitatively dependent on the changed model parameters.

Drying is imposed by a relaxation of the model's specific humidity field toward zero in a given layer, whose boundaries in pressure are p_1 and p_2. This can be thought of as a crude representation of horizontal advection of dry air, where the relaxation time scale is a length scale associated with horizontal moisture gradients divided by a typical horizontal velocity. Here we impose the strength of the humidity removal either by specifying its total integral F_q (in kg m^{-2} s^{-1} or W m^{-2}) or by specifying the relaxation time scale τ_q. Thus, the imposed horizontal advective drying $\partial_t q(p,t)\,|_{\text{hadv}}$ is

$$\partial_t q(p,t)|_{\text{hadv}} = -\frac{q(p,t)}{\tau_q} \quad \text{for } p_1 < p < p_2, \quad \text{where} \tag{1}$$

$$\tau_q = F_q^{-1} \int_{p_1}^{p_2} Lq \frac{dp}{g}, \tag{2}$$

L is the latent heat of vaporization, and g is the acceleration of gravity, with F_q given in W m^{-2}. Either F_q or τ_q can be specified but not both, since they are related through the model solution for q which is not known a priori.

A result of our calculations shown below is that in each model, the functional relationship between F_q and τ_q is almost exactly the same regardless of which one of them is specified (see Fig. 7). It is not entirely obvious that this need be the case—feedbacks involving the q field could conceivably change the relationship when the model formulation is changed via the imposition of F_q instead of τ_q or vice versa—but the fact that it is simplifies the presentation and interpretation of the results. Most results are presented only in terms of F_q, and where not stated otherwise the results shown are for the calculations for which F_q is fixed (although again the results are essentially the same for the fixed τ_q results, as long as they are compared at constant F_q).

A valid quasi-steady model solution can be obtained for a positive and sufficiently large τ_q. At a bare minimum τ_q must be greater than the model time step; in practice, the effective minimum we find is usually greater than that. In physical terms, for τ_q below the minimum, the drying removes moisture faster than the other processes represented in the model can resupply it. This means that for any given model, set of boundary conditions, and choice of p_1 and p_2, there is a threshold value of F_q such that steady solutions cannot be obtained for F_q larger than that threshold. We will show below that the threshold value for F_q is quite variable depending on which model we choose and the values for p_1 and p_2, but it tends to be on the order of tens of W m^{-2}, smaller with smaller values of p_1 and p_2 (drying at higher levels), and smaller in the MIT than in the GEOS5 model.

We perform three sets of experiments with each model, with export of humidity from the upper (p_1 = 150 hPa, p_2 = 375 hPa), middle (p_1 = 375 hPa, p_2 = 600 hPa), and lower free troposphere (p_1 = 600 hPa, p_2 = 825 hPa).

The GEOS5 model is run for 6 months, with all plotted quantities shown as averages over the last month. The

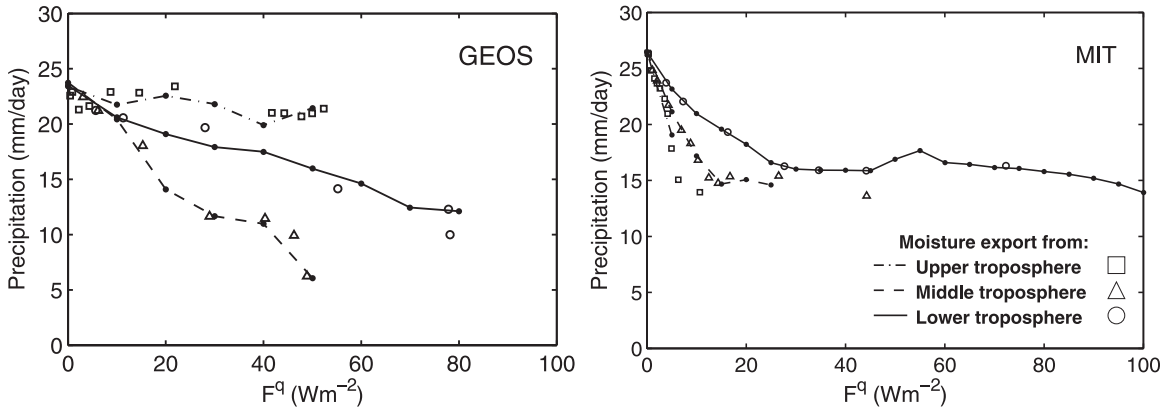

FIG. 3. Equilibrium precipitation as a function of the humidity export in the upper, middle, and lower free troposphere for simulations with a constant flux F_q (curves) and constant drying time scale τ_q (open symbols) in both models: (left) GEOS and (right) MIT.

MIT model is run for 300 days, and plotted quantities are averages over the last 100 days. Both models undergo small- to moderate-amplitude oscillations in some cases. In the GEOS5 model the period of these oscillations does not exceed 3–4 days. It can be on the order of 10 days in the MIT model, motivating the longer averaging time in that model.

4. Results

a. Precipitation, humidity, and vertical velocity

Figure 3 shows the precipitation in both models as a function of F_q. Results are shown for the calculations with fixed F_q as well as with fixed τ_q, demonstrating that there is little difference in the results as long as they are compared at equal F_q. Results are shown for the values of F_q at which statistically steady solutions were obtained. In the MIT model in particular, we see that the threshold past which solutions cannot be obtained occurs at relatively small F_q for export in the middle and especially the upper troposphere. Precipitation tends to decrease with F_q, although this is not true everywhere and there are large ranges where the dependence of precipitation on F_q is very weak. Perhaps most significant is the result that in both models, dry air injection in the middle troposphere is more effective, per W m^{-2}, at suppressing precipitation than is dry air injection in the lower troposphere. The response of the two models to dry air injection in the upper troposphere is very different: in the MIT model the precipitation is reduced drastically by the injection of dry air, leading to the suppression of convection for small F_q; in the GEOS5 model, the precipitation is insensitive to the export of humidity from the upper troposphere.

Figures 4 and 5 show the pressure vertical velocity ω and relative humidity as functions of pressure and F_q. We see dramatic differences in ω between the two models. The GEOS5 model ω tends to exceed that from the MIT model by close to an order of magnitude and has strong ascent in the upper to midtroposphere, around the 400–500-hPa layer, with strong descent below, whereas the MIT model has ascent throughout the troposphere. This is a large difference.

The relative humidity field shows large differences as well. The MIT model is much drier throughout the troposphere than is the GEOS5 model, except right around the tropopause where the former approaches saturation.

Figure 6 shows precipitation in both models as a function of τ_q, with the latter on a logarithmic scale. In both models, drying in the upper troposphere is relatively ineffective at suppressing precipitation when compared in this way to middle- and lower-tropospheric drying. For values of τ_q less than 10–20 days, dry air injection in the middle and lower troposphere is more effective. In the MIT model, lower tropospheric drying is more effective for larger τ_q, but middle tropospheric drying becomes approximately equally effective around $\tau_q = 5$ days and below. In the GEOS5 model, lower and middle tropospheric drying have similar effects down to 5 days, the smallest value for which a precipitating, quasi-steady state can be reached, with middle tropospheric drying being slightly more effective over much of the range shown.

These results are to some degree consistent with our expectation that dry air in the lower troposphere may inhibit deep convection more effectively than in the upper troposphere. Perhaps more surprising is that middle-tropospheric drying is equally or more effective than lower-tropospheric drying even using fixed τ_q as a basis for comparison. The same τ_q corresponds to smaller F_q in the middle troposphere than in the lower troposphere.

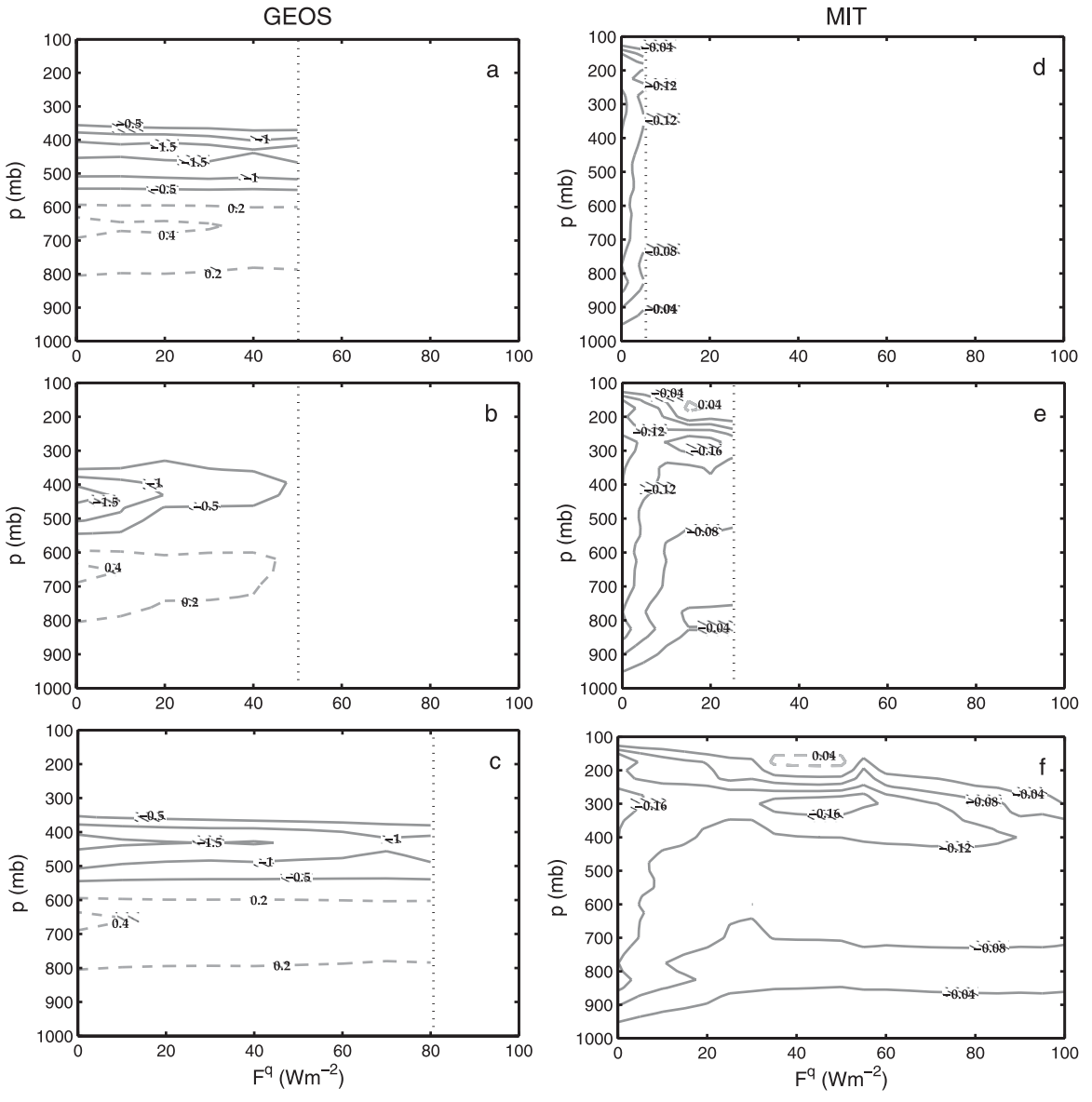

FIG. 4. Equilibrium pressure vertical velocity ω (Pa s^{-1}) as a function of the humidity export in the (top) upper, (middle) middle, and (bottom) lower free troposphere for simulations with a constant flux F_q in both models: (left) GEOS and (right) MIT. Solid (dashed) contours indicate negative (positive) values.

Figure 7 shows the relationships between F_q and τ_q in both models for drying imposed in the different vertical layers. (These relationships are implicit in Figs. 3 and 6 but are difficult to ascertain from inspection of those figures.) Again, there are clear differences between the two models, particularly at small τ_q. In the GEOS5 results, and in the MIT model results at large τ_q, F_q is approximately inversely proportional to τ_q. This indicates that the total water vapor in the layer in which the drying is applied does not vary much; apparently it is tightly controlled by convection, vertical advection, or a combination of the two. At small τ_q, the MIT model departs significantly from this behavior, indicating a stronger influence of the drying on the humidity field.

Figure 8 shows relationships between the precipitation and column-integrated saturation fraction, defined as the ratio of the column-integrated precipitable water to its saturation value, for both models. This has proven a useful diagnostic in observational (Bretherton et al. 2004) and modeling studies (Raymond 2007). Points from both the fixed-τ_q and fixed-F_q calculations are shown. The

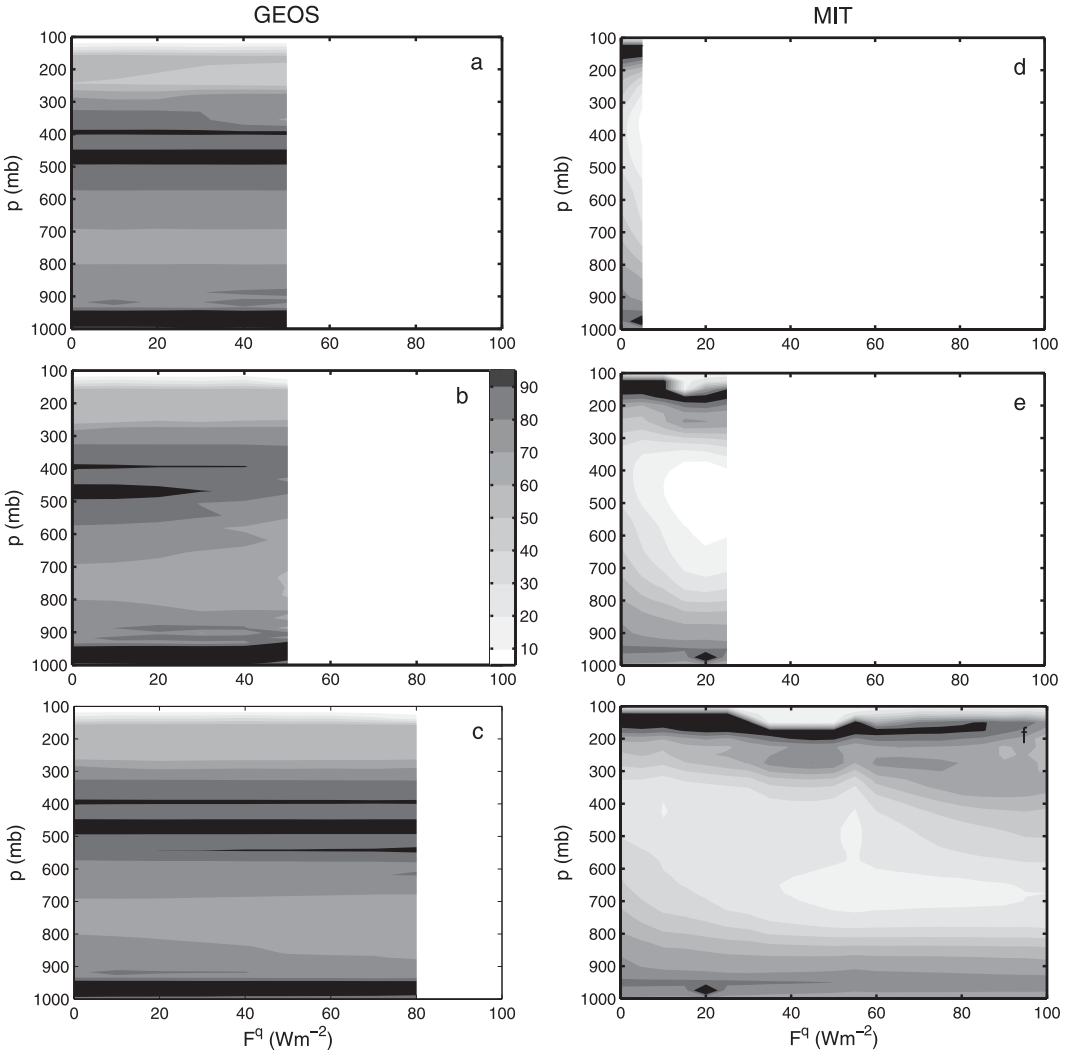

FIG. 5. As in Fig. 4, but for equilibrium relative humidity (%).

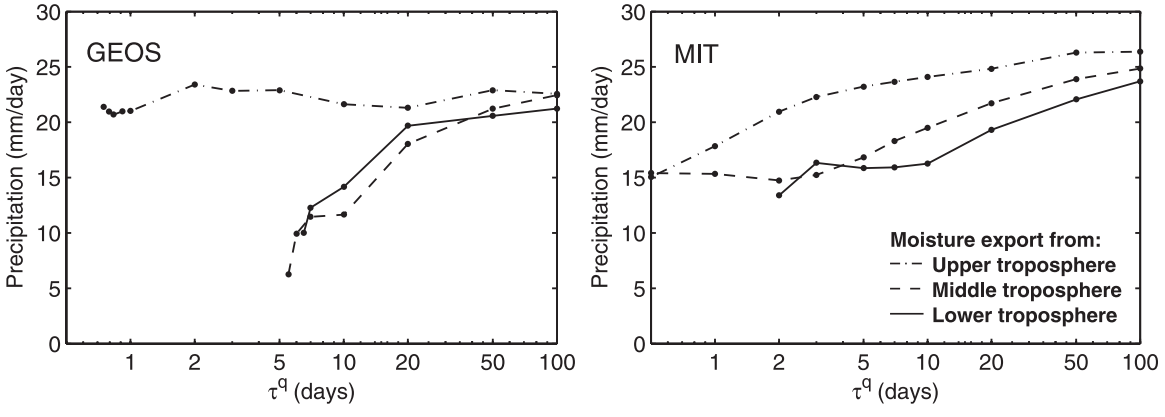

FIG. 6. Precipitation as a function of the humidity export in in the (top) upper, (middle) middle, and (bottom) lower free troposphere for simulations with a constant relaxation time τ_q in both models: (left) GEOS and (right) MIT.

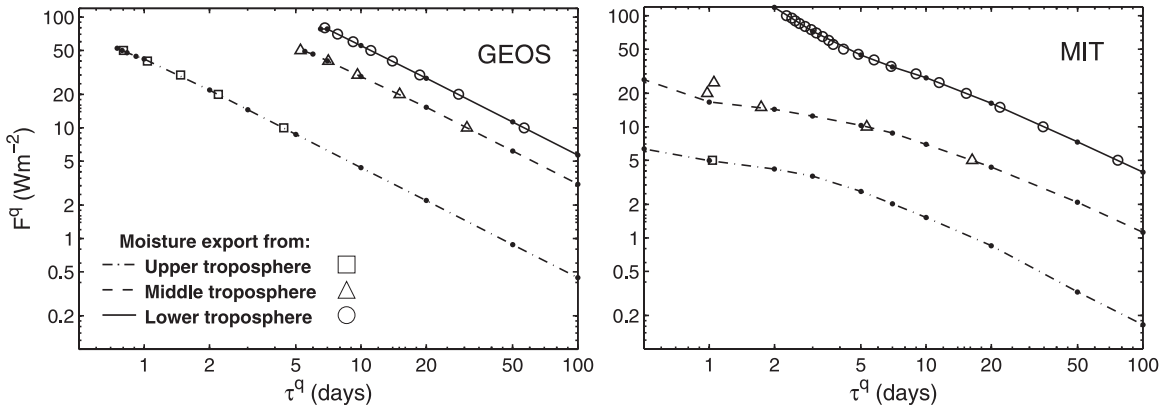

FIG. 7. Humidity flux F_q vs drying time scale τ_q for simulations with a constant flux Fq (curves) and constant drying time scale τ_q (open symbols) in both models: (left) GEOS and (right) MIT.

difference between the two models is striking, with the MIT model being much drier (as also seen in Fig. 5), exhibiting a shallower slope and also exhibiting more significant outliers from otherwise compact relationships than does the GEOS5 model. Our experiment design might perhaps be expected to generate outliers because by forcing the humidity field in different layers we deliberately attempt to exercise multiple degrees of freedom in the humidity profile, whereas the column-integrated diagnostic addresses only one.

b. *Moist static energy budget*

Figure 9 shows the terms in the vertically integrated moist static energy budget for both models as functions of F_q. Including F_q itself (which is not shown explicitly), the budgets balance in both models to within a fraction of a W m^{-2}. Focusing first on the calculations with lower tropospheric drying, we see that the two models arrive at similar precipitation rates with very different moist static energy budgets. The MIT model has substantially larger latent heat flux than GEOS5 for all F_q. At $F_q = 0$ this is compensated for by somewhat larger radiative cooling and (vertical) advective export of moist static energy. The dependence on F_q as the latter increases is then strikingly different. In the GEOS5 model, all terms but the vertical advection remain close to constant whereas the vertical advection increases (decreasing in absolute value, representing decreasing export of moist static energy from the column) almost linearly, compensating approximately by itself for the imposed horizontal advective drying F_q. Between $F_q = 60$ and 70 W m^{-2}, the vertical advective tendency actually becomes positive, indicating a negative gross moist stability (Neelin and Held 1987). In the MIT model, for $F_q < 55$ W m^{-2} the vertical advection stays roughly constant and then decreases (increases in absolute value) whereas the surface latent heat flux rises (to compensate partly for F_q) and the vertical advective changes, aided somewhat by smaller increases in radiative cooling in sensible heat flux. Thereafter the vertical advection

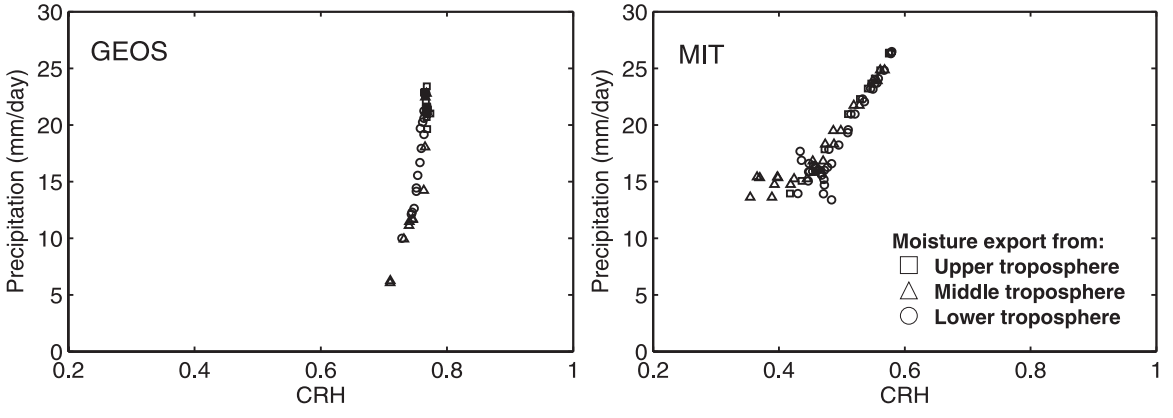

FIG. 8. Precipitation as a function of the column-integrated saturation fraction: (left) GEOS and (right) MIT.

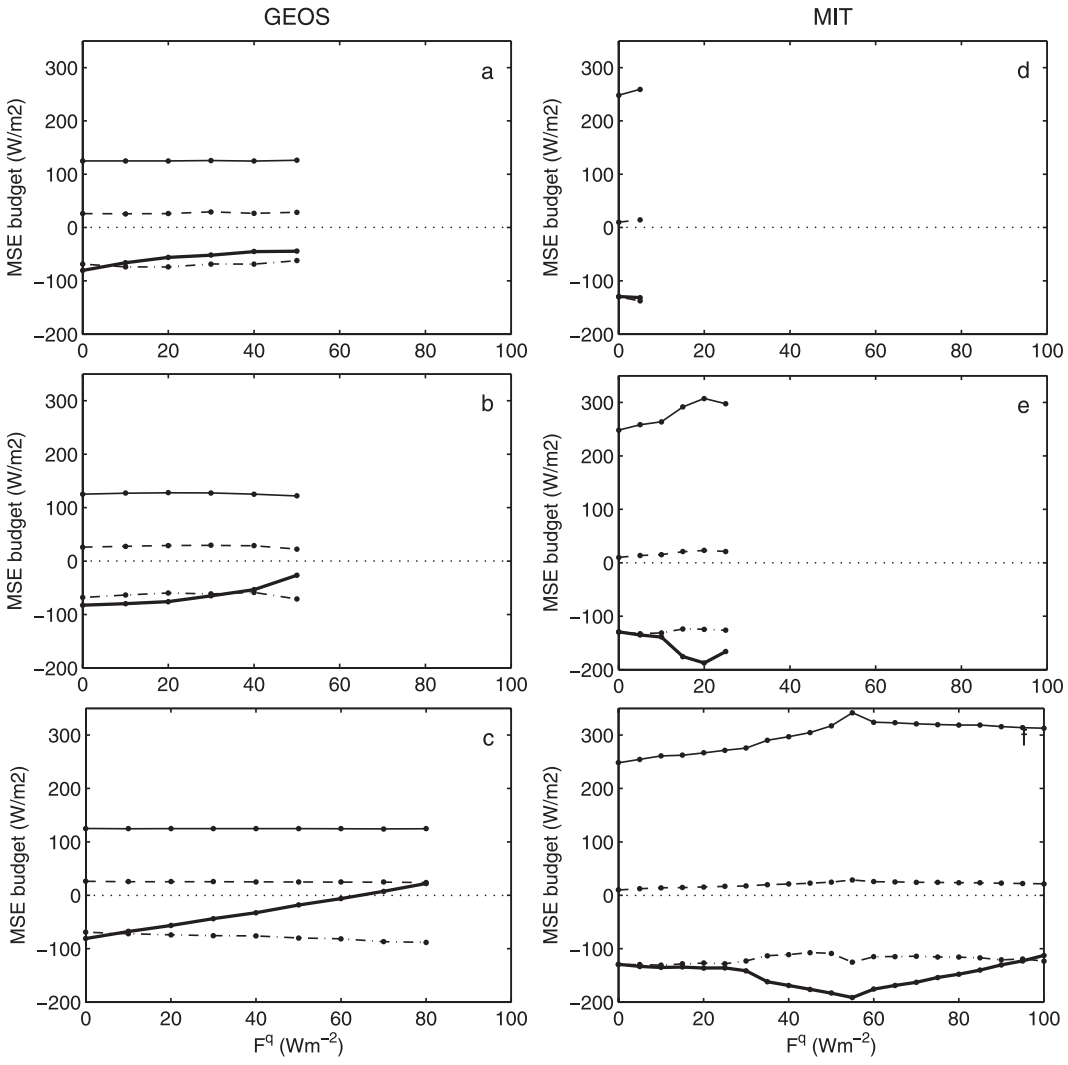

FIG. 9. Terms in the column-integrated moist static energy budget as a function of the humidity export in the (top) upper, (middle) middle, and (bottom) lower free troposphere for simulations with a constant flux F_q in both models: (left) GEOS and (right) MIT. Solid curves are the surface latent heat flux, dashed are the surface sensible heat flux, dashed–dotted are vertically integrated radiative heating, and thick lines are vertically integrated vertical advection.

increases (decreases in absolute value) and latent heat flux decreases weakly; past this point the behavior of the terms bears some resemblance to that in the GEOS5 model.

The moist static energy (MSE) budgets of the upper- and middle-tropospheric advection solutions resemble those of the lower-tropospheric solutions but extend over smaller ranges of F_q.

Figure 10 shows the ''gross moist stability ratio'' for the GEOS5 and MIT models for the calculations with F_q fixed. The gross moist stability ratio, or normalized gross moist stability (Raymond et al. 2007), is the vertical advective export of moist static energy from the column divided by the export of dry static energy:

$$M_R = \frac{\int \omega \frac{\partial h}{\partial p} dp}{\int \omega \frac{\partial s}{\partial p} dp}, \tag{3}$$

where ω is the vertical velocity, h is the moist static energy, s is dry static energy, and the integration in pressure p is over the entire depth of the atmosphere. Equation (3) gives a dimensionless number that is directly relevant to theories for precipitation. It is equivalent to the ratio of the gross moist stability to gross dry stability, as those are usually defined. In steady state and under standard approximations, the smaller the ratio M_R, the larger the precipitation, for fixed input of moist

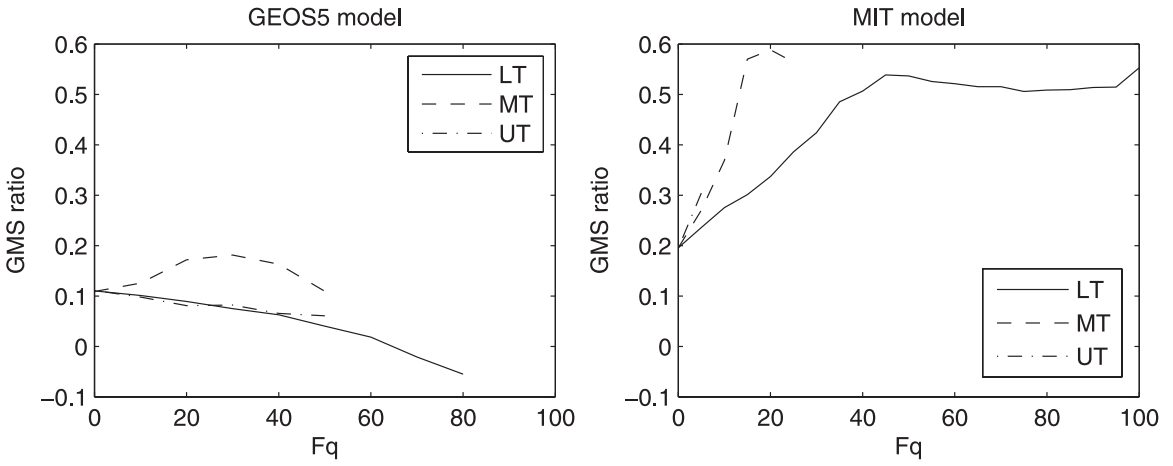

FIG. 10. Gross moist stability ratio in the (left) GEOS5 and (right) MIT models as a function of imposed drying F_q, when drying is imposed in the lower (LT), middle (MT), and upper troposphere (UT).

static energy to the column due to surface fluxes, radiation, and horizontal advection (e.g., Raymond et al. 2007).

The large difference between the two models is immediately evident in Fig. 10: M_R in the GEOS5 model is much smaller than in the MIT model for all F_q and becomes negative at large F_q. The difference is largely due to the very different profiles of ω, with the MIT model's profile implying (via mass conservation) relatively more inflow near the level of the moist static energy minimum and outflow at higher levels where the moist static energy is larger, so that the difference in moist static energy between air leaving and entering the column is larger than in the GEOS5 model [see Neelin (1997) or Sobel (2007) for discussions of the relationship between ω profiles and the gross moist stability]. The more humid atmosphere, and thus the shallower moist static energy minimum in the GEOS5 model, also plays a role. The difference in the gross moist stabilities is consistent with the much larger surface fluxes in the MIT model at comparable precipitation rates.

Increasing F_q in the lower troposphere decreases M_R in the GEOS5 model but increases it in the MIT model; F_q in the middle troposphere increases M_R in both models, at least for small F_q. In both models, a maximum is reached at a modest value of F_q, after which the ratio decreases again, although in the MIT model the inability to reach a steady solution occurs shortly after the maximum so that the decrease is only barely in evidence.

In theories for tropical precipitation, the gross moist stability (and the ratio M_R) is often either constant or simply parameterized as a function of vertically integrated state variables and is generally taken to be positive (e.g., Neelin and Held 1987; Neelin 1997; Neelin et al. 2003; Neelin 2007; Raymond 2000; Sobel and Gildor 2003; Bretherton and Sobel 2002). These assumptions are convenient and lead to a range of useful theoretical results, but they are questionable. The gross moist stability is very sensitive to the vertical profile of large-scale vertical velocity, which depends in a delicate and poorly constrained way on model physics (Sobel 2007). Back and Bretherton (2006) use observations to show that the gross moist stability of the time-averaged divergent flow may be negative in some regions of the tropics, and Frierson (2007) shows how different convective parameterizations lead to very different gross moist stabilities, and thus to different solutions, in a GCM.

Our results in Figs. 9 and 10 highlight this point further. In the first place, they show the strong model dependence of M_R, consistent with previous work (Frierson 2007). The results also show that at least in these models, the gross moist stability is not at all fixed; rather, it can be a strong function of the external forcing, here F_q. In the GEOS5 model, for example, the gross moist stability adjusts to imposed drying so that the drying is approximately compensated by opposite changes in vertical advection of moist static energy. Further, the results show how the same F_q—the same net advective forcing of the moist static energy budget in a column integral—can have quite different effects depending on the level at which the forcing is applied.

5. Conclusions

We have used two single-column models run in weak temperature gradient mode to examine the sensitivity of parameterized deep convection to imposed advective drying in different vertical layers. The main findings are as follows:

1) Under the same forcings, the two models reach very different solutions. Even when adjustments are made so that the precipitation rates are similar, other aspects of the solutions remain very different.
2) In both models, drying at midlevels is equally or more effective than drying at lower levels in suppressing deep convection.

The fact that the second conclusion holds true in two very different sets of solutions from two models, and for two different ways of comparing the results of different experiments (fixed F_q versus fixed τ_q), is provocative. It is possible that lower-tropospheric drying is rendered more ineffective than it should be in both models because of inadequate entrainment of lower-tropospheric air in the parameterized convection, as has been argued is generically the case for a wide range of existing convective parameterizations (e.g., Derbyshire et al. 2004; Kuang and Bretherton 2006). Other flaws in the parameterizations, such as incorrect response to buoyancy perturbations, could also influence the results. It would be desirable to carry out similar experiments with cloud-resolving models.

That differences occur in the model solutions between the two models may not be surprising, but the magnitudes of the differences are large compared with those found between different models in more constrained simulations. The WTG framework, with its feedbacks between parameterized dynamics and physics, may allow more dramatic differences between models to emerge than do so in radiative–convective equilibrium or in simulations with imposed vertical advective tendencies (Ghan et al. 2000; Bechtold et al. 2000; Xie et al. 2002; Randall et al. 2003).

Acknowledgments. We thank Kerry Emanuel and Sandrine Bony for help with the MIT model and Julio Bacmeister for help with GEOS5. This work was supported by NASA Grant NNX06AB48G.

APPENDIX

Parameter Changes in the MIT Model

The key parameters we change in the MIT model are σ_D, the fractional area of convective downdrafts; σ_s, the fraction of the rain shaft falling through the environment; and α, which is the rate at which the convective mass flux is relaxed toward its equilibrium value. The control MIT model has $\alpha = 0.02$, $\sigma_D = 0.05$, and $\sigma_s = 0.12$. The modified model has $\alpha = 0.2$, $\sigma_D = 0.02$, and $\sigma_s = 0.06$.

REFERENCES

Back, L. E., and C. S. Bretherton, 2006: Geographic variability in the export of moist static energy and vertical motion profiles in the tropical Pacific. *Geophys. Res. Lett.,* **33,** L17810, doi:10.1029/2006GL026672.

Bechtold, P., and Coauthors, 2000: A GCSS model intercomparison for a tropical squall line observed during TOGA COARE. II: Intercomparison of single-column models and a cloud-resolving model. *Quart. J. Roy. Meteor. Soc.,* **126,** 865–888.

Biasutti, M., A. H. Sobel, and Y. Kushnir, 2006: GCM precipitation biases in the tropical Atlantic. *J. Climate,* **19,** 935–958.

Bony, S., and K. A. Emanuel, 2001: A parameterization of the cloudiness associated with cumulus convection: Evaluation using TOGA COARE data. *J. Atmos. Sci.,* **58,** 3158–3183.

——, C. Risi, and F. Vimeux, 2008: Influence of convective processes on the isotopic composition (δ^{18}O and δD) of precipitation and water vapor in the tropics. 1. Radiative–convective equilibrium and Tropical Ocean–Global Atmosphere Coupled Ocean–Atmosphere Response Experiment (TOGA COARE) simulations. *J. Geophys. Res.,* **113,** D19305, doi:10.1029/2008JD009942.

Bretherton, C. S., 2007: Challenges in numerical modeling of tropical circulations. *The Global Circulation of the Atmosphere,* T. Schneider and A. H. Sobel, Eds., Princeton University Press, 302–330.

——, and A. H. Sobel, 2002: A simple model of a convectively coupled Walker circulation using the weak temperature gradient approximation. *J. Climate,* **15,** 2907–2920.

——, M. E. Peters, and L. E. Back, 2004: Relationships between water vapor path and precipitation over the tropical oceans. *J. Climate,* **17,** 1517–1528.

Brown, R. G., and C. Zhang, 1997: Variability of midtropospheric moisture and its effect on cloud-top height distribution during TOGA COARE. *J. Atmos. Sci.,* **54,** 2760–2774.

Cetrone, J., and R. A. Houze, 2006: Characteristics of tropical convection over the ocean near Kwajalein. *Mon. Wea. Rev.,* **134,** 834–853.

Chiang, J. C. H., and A. H. Sobel, 2002: Tropical tropospheric temperature variations caused by ENSO and their influence on the remote tropical climate. *J. Climate,* **15,** 2616–2631.

Chou, M.-D., and M. J. Suarez, 1999: A solar radiation parameterization (CLIRAD-SW) for atmospheric studies. NASA Tech. Memo. 10460, 38 pp.

Derbyshire, S. H., I. Beau, P. Bechtold, J.-Y. Grandpeix, J.-M. Piriou, J.-L. Redelsperger, and P. M. Soares, 2004: Sensitivity of moist convection to environmental humidity. *Quart. J. Roy. Meteor. Soc.,* **130,** 3055–3080.

Emanuel, K. A., 1991: A scheme for representing cumulus convection in large-scale models. *J. Atmos. Sci.,* **48,** 2313–2329.

——, and M. Zivkovic-Rothman, 1999: Development and evaluation of a convection scheme for use in climate models. *J. Atmos. Sci.,* **56,** 1766–1782.

Fouquart, Y., and B. Bonnel, 1980: Computation of solar heating of the earth's atmosphere: A new parameterization. *Beitr. Phys. Atmos.,* **53,** 35–62.

Frierson, D. M. W., 2007: The dynamics of idealized convection schemes and their effect on the zonally averaged tropical circulation. *J. Atmos. Sci.,* **64,** 1959–1976.

Ghan, S., and Coauthors, 2000: An intercomparison of single-column model simulations of summertime midlatitude continental convection. *J. Geophys. Res.,* **105,** 2091–2124.

Kuang, Z., and C. S. Bretherton, 2006: A mass flux scheme view of a high-resolution simulation of a transition from shallow to deep cumulus convection. *J. Atmos. Sci.,* **63,** 1895–1909.

Lin, J.-L., and Coauthors, 2006: Tropical intraseasonal variability in 14 IPCC AR4 climate models. Part I: Convective signals. *J. Climate,* **19,** 2665–2690.

Mapes, B. E., and P. Zuidema, 1996: Radiative–dynamical consequences of dry tongues in the tropical troposphere. *J. Atmos. Sci.,* **53,** 620–638.

Moorthi, S., and M. J. Suarez, 1992: Relaxed Arakawa–Schubert: A parameterization of moist convection for general circulation models. *Mon. Wea. Rev.,* **120,** 978–1002.

Morcrette, J.-J., 1991: Radiation and cloud radiative properties in the European Centre for Medium-Range Weather Forecasts forecasting system. *J. Geophys. Res.,* **96,** 9121–9132.

Neelin, J. D., 1997: Implications of convective quasi-equilibrium for the large-scale flow. *The Physics and Parameterization of Moist Atmospheric Convection,* R. K. Smith, Ed., Kluwer Academic, 413–446.

——, 2007: Moist dynamics of tropical convection zones in monsoons, teleconnections, and global warming. *The Global Circulation of the Atmosphere,* T. Scneider and A. H. Sobel, Eds., Princeton University Press, 267–301.

——, and I. M. Held, 1987: Modeling tropical convergence based on the moist static energy budget. *Mon. Wea. Rev.,* **115,** 3–12.

——, C. Chou, and H. Su, 2003: Tropical drought regions in global warming and El Niño teleconnections. *Geophys. Res. Lett.,* **30,** 2275, doi:10.1029/2003GL018625.

Parsons, D., and Coauthors, 1994: The Integrated Sounding System: Description and preliminary observations from TOGA COARE. *Bull. Amer. Meteor. Soc.,* **75,** 553–567.

Peters, O., and J. D. Neelin, 2006: Critical phenomena in atmospheric precipitation. *Nat. Phys.,* **2,** 393–396, doi:10.1038/nphys314.

Randall, D. A., M. Khairoutdinov, A. Arakawa, and W. W. Grabowski, 2003: Breaking the cloud parameterization deadlock. *Bull. Amer. Meteor. Soc.,* **84,** 1547–1564.

Raymond, D. J., 2000: Thermodynamic control of tropical rainfall. *Quart. J. Roy. Meteor. Soc.,* **126,** 889–898.

——, 2007: Testing a cumulus parametrization with a cumulus ensemble model in weak-temperature-gradient mode. *Quart. J. Roy. Meteor. Soc.,* **133,** 1073–1085.

——, and X. Zeng, 2005: Modeling tropical atmospheric convection in the context of the weak temperature gradient approximation. *Quart. J. Roy. Meteor. Soc.,* **131,** 1301–1320.

——, G. Raga, C. S. Bretherton, J. Molinari, C. López-Carrillo, and Z. Fuchs, 2003: Convective forcing in the intertropical convergence zone of the eastern Pacific. *J. Atmos. Sci.,* **60,** 2064–2082.

——, S. Sessions, and Z. Fuchs, 2007: A theory for the spinup of tropical depressions. *Quart. J. Roy. Meteor. Soc.,* **133,** 1743–1754.

Rennó, N. O., K. A. Emanuel, and P. H. Stone, 1994a: Radiative-convection model with an explicit hydrologic cycle. 1: Formulation and sensitivity to model parameters. *J. Geophys. Res.,* **99,** 14 429–14 441.

——, P. H. Stone, and K. A. Emanuel, 1994b: Radiative-convection model with an explicit hydrologic cycle. 2: Sensitivity to large changes in solar forcing. *J. Geophys. Res.,* **99,** 17 001–17 020.

Sherwood, S. C., 1999: Convective precursors and predictability in the tropical western Pacific. *Mon. Wea. Rev.,* **127,** 2977–2991.

——, and R. Wahrlich, 1999: Observed evolution of tropical deep convective events and their environment. *Mon. Wea. Rev.,* **127,** 1777–1795.

Sobel, A. H., 2007: Simple models of ensemble-averaged tropical precipitation and surface wind, given the sea surface temperature. *The Global Circulation of the Atmosphere,* Princeton University Press, 219–251.

——, and C. S. Bretherton, 2000: Modeling tropical precipitation in a single column. *J. Climate,* **13,** 4378–4392.

——, and H. Gildor, 2003: A simple time-dependent model of SST hot spots. *J. Climate,* **16,** 3978–3992.

——, S. E. Yuter, C. S. Bretherton, and G. N. Kiladis, 2004: Large-scale meteorology and deep convection during TRMM KWAJEX. *Mon. Wea. Rev.,* **132,** 422–444.

——, G. Bellon, and J. Bacmeister, 2007: Multiple equilibria in a single-column model of the tropical atmosphere. *Geophys. Res. Lett.,* **34,** L22804, doi:10.1029/2007GL031320.

Straub, K. H., and G. N. Kiladis, 2002: Observations of a convectively coupled Kelvin wave in the eastern Pacific ITCZ. *J. Atmos. Sci.,* **59,** 30–53.

——, and ——, 2003: The observed structure of convectively coupled Kelvin waves: Comparison with simple models of coupled wave instability. *J. Atmos. Sci.,* **60,** 1655–1668.

Tokioka, T., K. Yamazaki, A. Kitoh, and T. Ose, 1988: The equatorial 30–60-day oscillation and the Arakawa–Schubert penetrative cumulus parameterization. *J. Meteor. Soc. Japan,* **66,** 883–901.

Xie, S., and Coauthors, 2002: Intercomparison and evaluation of cumulus parameterizations under summertime midlatitude continental conditions. *Quart. J. Roy. Meteor. Soc.,* **128,** 1095–1135.

Yoneyama, K., and T. Fujitani, 1995: The behavior of the dry westerly air associated with convection observed during the TOGA COARE R/V *Natsushima* cruise. *J. Meteor. Soc. Japan,* **73,** 291–304.

Zhang, C., B. E. Mapes, and B. J. Soden, 2003: Bimodality in tropical water vapor. *Quart. J. Roy. Meteor. Soc.,* **129,** 2847–2866.